Zinc Binding to the HIV-1 Nucleocapsid Protein: A Thermodynamic Investigation by Fluorescence Spectroscopy†

Y. Mély,*,‡ H. De Rocquigny,§ N. Morellet,§ B. P. Roques,§ and D. Gérard‡

Laboratoire de Biophysique, URA 491 du CNRS, Faculté de Pharmacie de Strasbourg I, B.P. 24, 67401 Illkirch Cedex, France, and Département de Chimie Organique, INSERM U266, CNRS UA 498, U. F. R. des Sciences Pharmaceutiques et Biologiques, 4, Avenue de l'Observatoire, 75270 Paris Cedex, France

Received October 31, 1995; Revised Manuscript Received January 19, 1996⊗

ABSTRACT: The HIV-1 nucleocapsid protein, NCp7, is characterized by two CCHC zinc finger motifs which have been shown to stoichiometrically bind zinc in mature virions. Moreover, this binding of zinc proves to be critical in various NCp7 functions, especially in the encapsidation process. To further understand the central role of zinc binding to NCp7, we closely investigated the zinc binding properties of NCp7 and various deleted or substituted derivatives. To this end, the fluorescence of either the naturally occurring Trp^{37} or the conservatively substituted Trp^{16} was used to monitor the binding of zinc to the N- and C-terminal finger motifs, respectively. At pH 7.5, the NCp7 proximal motif was found to bind zinc strongly with a 2.8×10^{14} M^{-1} binding constant about five times higher than the NCp7 distal motif. Moreover, the binding of zinc to one finger motif decreased the affinity of the second one, and this negative cooperativity was shown to be related to the spatial proximity of the zinc-saturated finger motifs. The binding seemed to be almost equally driven by entropy and enthalpy, and the binding information was essentially encoded by the finger motifs themselves whereas the other parts of the protein only played a marginal stabilization role. As expected, the Cys and His residues of the CCHC motifs were critical and competition between protons and zinc ions to these residues induced a steep pH-dependence of the zinc binding constants to both sites. Taken together, our data provide further evidence for the nonequivalence of the two NCp7 finger motifs.

Like all retroviruses, the human immunodeficiency virus type 1 (HIV-1)[1] encodes a *gag* gene product that is processed by the retroviral protease to give several structural proteins including the matrix, capsid and nucleocapsid protein (NC). The final mature NC product, NCp7, is a small basic protein containing two copies of a conserved zinc finger-like domain with the sequence Cys-X_2-Cys-X_4-His-X_4-Cys, called the CCHC motif (Berg, 1986). Both finger domains of NCp7 coordinate one zinc ion in mature virus preparations (Bess et al., 1992; Summers et al., 1992). This binding of zinc folds the finger domains into a stable and similar constrained structure (Omichinski et al., 1991; Morellet et al., 1992; Summers et al., 1992) and brings them spatially close together (Morellet et al., 1992, 1994; Mély et al., 1994).

In the virion, NC stabilizes RNA in a histone-like manner (Karpel et al., 1987) whereas, in the host cell, the NC sequence of the Gag polyprotein precursor is critically involved in the specific binding to the genomic RNA encapsidation sequence ψ (Berkowitz et al., 1993; Sakaguchi et al., 1993; Berkowitz & Goff, 1994; Dannull et al., 1994; Clever et al., 1995). This binding step, thought to be one of the primary events in the selective encapsidation of viral genomic RNA from the pool of cellular RNAs (Darlix et al., 1995, and references therein), is critically dependent on both the binding of zinc to the CCHC motifs and the *bona fide* conformation of NC since deletions or point mutations in either CCHC motif impair the *in vitro* binding to genomic ψ elements (Morellet et al., 1992; Berkowitz et al., 1993; Berkowitz & Goff, 1994; Dannull et al., 1994; Déméné et al., 1994; Ottmann et al., 1995) and strongly decrease the packaging of genomic RNA, giving rise to poorly infectious viral particles (Aldovini & Young, 1990; Gorelick et al., 1990; Dorfman et al., 1993; Déméné et al., 1994; Ottmann et al., 1995). Interestingly, C-nitroso compounds acting as zinc-depleting agents strongly decrease the HIV-1 infectivity and are thus proposed as potential therapeutic compounds (Rice et al., 1993).

In contrast, other *in vitro* reported NCp7 activities such as activation of retroviral RNA dimerization (Darlix et al., 1990), $tRNA^{Lys,3}$ annealing to the initiation site of reverse transcription (Barat et al., 1989, 1991) and strong stop cDNA annealing to the 3′ end of the genomic RNA (Lapadat-Tapolsky et al., 1993) seem to be not strictly dependent on the presence of zinc-saturated finger motifs (De Rocquigny et al., 1992; Lapadat-Tapolsky et al., 1995).

Despite their strong structural similarities, the two zinc-saturated finger domains of NCp7 seem to be not thermodynamically and functionally equivalent. Indeed, NMR and Co^{2+}-binding studies suggest that the affinities of the two motifs for zinc are probably not identical (De Rocquigny et al., 1991; Fitzgerald & Coleman, 1991), and the zinc-saturated C-terminal motif shows a higher conformational lability than the N-terminal one (South et al., 1991; Déméné

† This work was supported by grants from the Agence Nationale de la Recherche sur le SIDA, Centre National de la Recherche Scientifique, and Université Louis Pasteur.

* Author to whom proofs and correspondence should be addressed.
‡ Faculté de Pharmacie de Strasbourg I.
§ U.F.R. des Sciences Pharmaceutiques et Biologiques.

⊗ Abstract published in *Advance ACS Abstracts,* April 15, 1996.

[1] Abbreviations: HIV-1, human immunodeficiency virus type 1; NC, nucleocapsid protein; Hepes, *N*-(2-hydroxyethyl)piperazine-*N*′-2-ethanesulfonic acid; MoMuLV, Moloney murine leukemia virus.

0006-2960/96/0435-5175$12.00/0

	Motif 1		Motif 2		
1				72	
MQRGNFRNQRKNVK	CFNCGKEGHTARNC	RAP RKKG	CWKCGKEGHQMKDC	TERQANFLGKIWPSYKGRPGNFL	(1-72)NCp7
VK	CFNCGKEGHTARNC	RAP RKKG	CWKCGKEGHQMKDC	TERQANFLGKIWPSY	(13-64)NCp7
VK	CFNCGKEG**C**TARNC	RAP RKKG	CWKCGKEGHQMKDC	TERQANFLGKIWPSY	Cys^{23}(13-64)NCp7
VK	CFNCGKEGHTARN**S**	RAP RKKG	CWKCGKEGHQMKDC	TERQANFLGKIWPSY	Ser^{28}(13-64)NCp7
VK	CFNCGKEGHTARNC	RA**P***RKKG	CWKCGKEGHQMKDC	TERQANFLGKIWPSY	D-Pro^{31}(13-64)NCp7
VK	C**W**NCGKEGHTARNC	RAP RKKG	C**F**KCGKEGHQMKDC	TERQANFLGKI**F**PSY	$Trp^{16}Phe^{37}Phe^{61}$(13-64)NCp7
MQRGNFRNQRKNVK	CFNCGKEGHTARNC	RAP RKKG	CWKCGKEGHQMKDC	TERQAN	(1-55)NCp7
NVK	CFNCGKEGHTARNC	RAP RKKG	CWKCGKEGHQMKDC	TERQ	(12-53)NCp7
NVK	C**Y**NCGKEGHTARNC	RAP RKKG	CWKCGKEGHQMKDC	TERQ	Tyr^{16}(12-53)NCp7
VK	C**W**NCGKEGHTARNC	RA			Trp^{16}(13-30)NCp7
		KG	CWKCGKEGHQMKDC	TE	(34-51)NCp7
				ERQANFLGKIWPSYKGRPGNFL	(51-72)NCp7

FIGURE 1: Amino acid sequences of NCp7 derivatives. Motifs 1 and 2 correspond to the N- and C-terminal zinc finger domains, respectively. P* refers to the D-Pro isomer. Mutated amino acids are represented by bold underlined letters.

et al., 1994). Moreover, the zinc-saturated N-terminal finger motif has been reported to be more critical than the C-terminal one for RNA encapsidation (Gorelick et al., 1990, 1993) and for specific binding to ψ-containing RNA sequences (Dannull et al., 1994). However, this strong preferential involvement of the N-terminal motif for specific binding is still controversial (Berkowitz et al., 1993 ; Berkowitz & Goff, 1994).

In this context, to further understand the central role of the binding of zinc in NCp7 functions, we closely investigated by fluorescence the zinc binding properties of NCp7 and various deleted or substituted derivatives. The pH- and temperature-dependence of the zinc binding parameters was also assessed to further complete the thermodynamic picture of the system.

MATERIALS AND METHODS

Materials. Solid phase synthesis of NCp7 and related peptides (Figure 1) was carried out as described (De Rocquigny et al., 1991). To preserve the highly oxidizable Cys residues, the lyophilized peptides were dissolved in freshly degassed buffer and immediately poured into anaerobic quartz cells, which maintained an inert argon atmosphere. The -SH content of the various peptides was checked at the beginning and the end of each experiment by titration with 5,5′-dithiobis(2-nitrobenzoic acid) (Cornille et al., 1990). To preserve the most oxidizable Cys^{23}(13−64)NCp7 derivative, 1 mM 2-mercaptoethanol was also added.

Spectroscopic Measurements. Absorption spectra were recorded on a Cary 4 spectrophotometer. Extinction coefficients of 5700, 7000, and 12 700 M^{-1} cm^{-1} at 280 nm were used for NCp7 derivatives either with one Trp, one Trp, and one Tyr or with two Trp and one Tyr, respectively.

To determine the experimental Zn^{2+} binding constants at 20 (±0.5) °C, fluorimetric titrations were performed with a thermostated SLM 48000 spectrofluorimeter by adding increasing zinc concentrations to a given peptide in 50 mM Hepes, 0.1 M KCl at the desired pH in the presence of 1 mM EDTA. For each addition of zinc, the fluorescence intensity changes at the maximum emission wavelength (353 nm) were followed for at least 30 min to ensure that equilibrium was attained. Excitation was set at 295 nm.

To investigate the pH-dependence of the experimental zinc binding constants, the buffer and the complexant were, respectively, MES (4-morpholineethanesulfonic acid) and EGTA for pH below 7, whereas Hepes and EDTA were used above pH 7. Three cells were monitored in parallel. In addition to 10 μM peptide, the three cells contained 1 mM complexant, 25 μM zinc, and a mixture of 0.5 mM zinc and 1 mM complexant, respectively. The same pH was adjusted in each cell with concentrated HCl or NaOH.

Similarly, the temperature-dependence over the 10−60 °C range of the experimental zinc binding constants was investigated with three cells (with the same composition as above) maintained in the thermostated compartment of the spectrofluorimeter. At each temperature, pH was adjusted to 7.5 with concentrated HCl or NaOH.

Quantum yields were determined by taking L-Trp in water ($\phi = 0.14$) as a reference (Eisinger & Navon, 1969).

Data Analysis: Determination of Experimental Zinc Binding Constants. In the case of peptides containing a single zinc finger motif, the average number, ν, of moles of zinc bound per mole of protein was determined from the fluorimetric titrations by: $\nu = (I - I_0)/(I_t - I_0)$, where I is the fluorescence measured for any added zinc concentration while I_0 and I_t correspond to the fluorescence intensities of the apopeptide and the fully zinc-saturated peptide, respectively. The concentration of free zinc, [Zn], was calculated using $[Zn] = [Zn_T]/[K_E([E_T] - [Zn_T])]$ where $[E_T]$ and $[Zn_T]$ designate, respectively, the total concentrations of complexant and zinc, while K_E is the affinity at a given temperature of the complexant for zinc calculated from Martell and Smith (1974) as described by Blinks et al. (1982). By using this equation, we made the reasonable assumption that the

Table 1: Quantum Yields and Zinc Binding Constants of NCp7 Derivatives at pH 7.5[a]

	Trp [b]	ϕ_0^{295}	$\phi_{1,1}^{295}$	ΔI_i [c]	k_1 (M^{-1})	k_2 (M^{-1})	k_3 (M^{-1})	$\Delta\Delta G$ [c] (kJ/mol)
(1−72)NCp7	37, 61	0.092 (±0.003)	0.153 (±0.006)	1.25	2.8 (±0.5) × 10^{14}	5.0 (±0.5) × 10^{13}	1.2 (±0.1) × 10^{13}	3.5
(13−64)NCp7	37, 61	0.092 (±0.004)	0.158 (±0.004)[f]	1.15	8 (±4) × 10^{13}	2.8 (±0.3) × 10^{13}	1.6 (±0.2) × 10^{13}	1.4
Cys^{23}(13−64)NCp7	37, 61	0.076 (±0.003)	0.130 (±0.003)[g]	1.0	1.0 (±0.5) × 10^{13}	2.6 (±0.4) × 10^{13}	3.5 (±0.8) × 10^{13}	−0.7
Ser^{28}(13−64)NCp7	37, 61	0.099 (±0.004)	0.170 (±0.005)	1.0		2.8 (±0.2) × 10^{13}		
D-Pro^{31}(13−64)NCp7	37, 61	0.093 (±0.003)	0.168 (±0.003)	1.0	7 (±3) × 10^{13}	2.9 (±0.2) × 10^{13}	2.8 (±0.5) × 10^{13}	<0.1
$Trp^{16}Phe^{37}Phe^{61}$(13−64)NCp7	16	0.056 (±0.002)	0.125 (±0.004)	1.72	1.2 (±0.1) × 10^{14}	5 (±2) × 10^{13}	1.7 (±0.5) × 10^{13}	2.6
(1−55)NCp7	37	0.060 (±0.002)	0.183 (±0.003)	1.20	3.5 (±0.9) × 10^{14}	1.7 (±0.2) × 10^{13}	1.3 (±0.1) × 10^{13}	0.7
(12−53)NCp7	37	0.064 (±0.003)	0.185 (±0.003)[e]	1.18	5 (±2) × 10^{13}	1.8 (±0.1) × 10^{13}	1.2 (±0.1) × 10^{13}	1.0
Tyr^{16}(12−53)NCp7	37	0.062 (±0.002)	0.182 (±0.004)[e]	1.21	4 (±2) × 10^{13}	1.8 (±0.2) × 10^{13}	1.0 (±0.1) × 10^{13}	1.4
Trp^{16}(13−30)NCp7	16	0.062 (±0.001)	0.175 (±0.004)[d]		5.7 (±0.3) × 10^{13}			
(34−51)NCp7	37	0.058 (±0.002)	0.207 (±0.004)[d]			1.7 (±0.1) × 10^{13}		

[a] Quantum yields (ϕ_0^{295} in the absence of zinc and $\phi_{1,1}^{295}$ in the presence of an excess of zinc) and association binding constants were reported as means (± standard error of the mean) for at least six and three experiments, respectively. [b] Trp position in amino acid sequence. [c] The fractional fluorescence change, ΔI_i, and the free energy of interaction, $\Delta\Delta G$, between the binding sites were calculated as described in the text. [d−f] Values from Mély et al. (1993b, 1994) and Morellet et al. (1994), respectively. [g] The value of Cys^{23}(13−64)NCp7 was slightly different from that previously reported (Morellet et al., 1994) because in the latter case, a slight oxidization occurred during zinc titration in the absence of 1 mM 2-mercaptoethanol.

concentrations of free zinc and zinc bound to the peptide were negligible in comparison to zinc bound to the complexant (EDTA or EGTA). The experimental zinc binding constant, k, was then computed by fitting the experimental values of ν and [Zn] to the equation $\nu = k[\mathrm{Zn}]/(1 + k[\mathrm{Zn}])$.

In the case of peptides containing two zinc finger motifs, the concentration of free zinc was calculated as above whereas the three independent binding constants, k_1 to k_3, were determined from eq 3 defined in the results section, using a non linear least-squares regression procedure of the SAS software.

Computational Simulation Procedures. To compare the hydration of the finger motifs in their apo- and holoforms, the Discover/NMRchitect software package from Biosym Technologies was used. The two peptides corresponding to the first and the second finger of NCp7 were first modeled in a extended conformation without zinc, using standard parameters for amino acids supplied with the Insight software package. These two peptides and the NMR-derived solution structure of the (12−53)NCp7 (Morellet et al., 1992) in its holoform were then surrounded by a layer of water of 5 Å. The resulting structures were then energy-minimized using a Lennard−Jones nonbond term and the Discover/amber force field. Non-bonded pair interactions were reduced to zero beyond a cutoff distance of 12 Å. Each structure was subjected to 40 000 steps of energy minimization, using a combination of steepest descent and conjugate gradient algorithms.

RESULTS

Strategy of NCp7 Derivative Synthesis. To examine at the molecular level the determinants of NCp7 zinc binding properties, several derivatives were synthesized. First of all, because two different major cleavage points of the precursor NCp15 by the HIV-1 protease have been reported depending on the HIV-1 isolate (BH10 or MN) considered (Sheng & Erikson-Viitanen, 1994), we synthesized two derivatives, (1−72)NCp7 and (1−55)NCp7, corresponding to these two cleavage products. Moreover, (13−64)NCp7 and (12−53)-NCp7 derivatives were prepared to analyze the role of the N- and C-terminal chains surrounding the central zinc finger domain. To specifically monitor the saturation of the proximal CCHC finger motif, a triply substituted $Trp^{16}Phe^{37}$-Phe^{61}(13−64)NCp7 (where the naturally occurring Phe^{16} was replaced by a Trp and the naturally occurring Trp^{37} and Trp^{61} were replaced by Phe residues) was synthesized. The ^{1}H NMR spectrum of this derivative (data not shown) and especially the presence of various long-range NOEs between protons of the proximal CCHC motif with those of the distal motif strongly suggested that the folding and the spatial proximity of the two zinc-saturated CCHC motifs were as in NCp7 (Morellet et al, 1994).

Furthermore, as substitution of any cysteine by a serine or mutation of His^{23} by Cys has been shown to impair the binding of NCp7 to genomic RNA and result in the production of non-infectious viruses (Gorelick et al., 1990; Dorfman et al., 1993; Dannull et al., 1994; Déméné et al., 1994), the zinc binding parameters of Ser^{28}(13−64)NCp7 and Cys^{23}(13−64)NCp7 were investigated. Similarly to check the incidence of the spatial proximity of the CCHC motifs on the zinc binding properties, Pro^{31} was substituted by D-Pro^{31} in (13−64)NCp7 since this substitution has been shown to impair the spatial proximity and to result in the formation of non-infectious viral particles (Morellet et al., 1994; Mély et al., 1994).

Finally, two 18-residue derivatives, Trp^{16}(13−30)NCp7 and (34−51)NCp7, corresponding to the amino acid sequences of the N- and C-terminal zinc finger domains (Figure 1), respectively, were synthesized to investigate the zinc binding properties of the isolated CCHC finger motifs.

Zinc Binding Parameters of the Isolated Zinc Finger Motifs. To monitor the binding of zinc to the (34−51)NCp7 derivative, the fluorescence of the naturally occurring Trp^{37} was used. As the corresponding aromatic amino acid in the N-terminal motif is the weakly fluorescent Phe^{16}, it was replaced by Trp. This substitution was not expected to modify the physicochemical properties of the peptide because the residue immediately following the first Cys in CCHC motifs is indifferently Phe or Trp in various related NCs and its nature does not affect the tertiary structure of the CCHC motif (Summers, 1991).

The fluorescence quantum yields of both Trp^{16}(13−30)-NCp7 and (34−51)NCp7 were sharply increased (by about 2.9- and 3.5-fold, respectively) in the presence of zinc. Using these large zinc-induced fluorescence changes, we measured in the presence of 1 mM EDTA (to buffer very low concentrations of free zinc) extremely high zinc binding affinities for both peptides (Table 1), in the same range as

those of the related NC of Rauscher (Green & Berg, 1990) or Moloney (Mély et al., 1991) murine leukemia virus. However, the binding constant of Trp^{16}(13−30)NCp7 was reproducibly 3-fold higher than the (34−51)NCp7 binding constant.

Steady-State Fluorescence Characterization of NCp7 Derivatives. In keeping with previous spectral data (Mély et al., 1993b, 1994) and the NMR-deduced structure of NCp7 (Omichinski et al., 1991; Morellet et al., 1992; Summers et al., 1992), the emission spectra of all derivatives exhibited a maximum emission wavelength at 351 (±1) and 353 (±1) nm for apo- and holoforms, respectively, suggesting a fully solvent exposition for Trp^{16}, Trp^{37}, or Trp^{61}. Moreover, in keeping with the high homology in the amino acid sequences of the two CCHC motifs and their random coil-type conformation in the absence of zinc (Summers, 1991), the quantum yields, ϕ_0, of Trp^{16} and Trp^{37} in various single Trp-containing apoderivatives were rather low and indistinguishable. Similarly, as expected, the quantum yield of apoderivatives containing both Trp^{37} and Trp^{61} residues corresponded to the average of the quantum yields of Trp^{37} in the apofinger motif and Trp^{61} in the fingerless Trp^{61}-containing (51−72)-NCp7 ($\phi = 0.121 \pm 0.003$) derivative.

As previously reported (Mély et al., 1994), the quantum yield, $\phi_{1,1}$, of holoderivatives strongly depends on the spatial proximity of the two zinc-saturated finger motifs. For derivatives with non interacting fingers [e.g., D-Pro^{31}(13−64)NCp7 and Ser^{28}(13−64)NCp7], the quantum yield of the holoderivatives simply corresponds to the arithmetic mean of the quantum yields of the (34−51)NCp7 holofinger motif and the fingerless Trp^{61}-containing (51−72) derivative. We thus inferred that the fluorescence of Trp^{37} was unaffected by the saturation of the proximal finger motif by zinc whereas Trp^{61} was unaffected by the binding of zinc to either finger motif in keeping with the almost structureless conformation of the C-terminal chain in the holoprotein (Morellet et al., 1994).

In contrast, holoderivatives with interacting fingers [e.g., (12−53)NCp7, (1−55)NCp7, (13−64)NCp7, $Trp^{16}Phe^{37}$-Phe^{61}(13−64)NCp7, (1−72)NCp7, ...] were characterized by a significantly lower quantum yield, $\phi_{1,1}$, than the corresponding derivatives (in term of Trp content and position) with non-interacting fingers. This decreased quantum yield has been correlated to additional collisions or radiationless relaxation processes due to the spatial proximity of the two zinc-saturated finger motifs (Mély et al., 1994).

Finally, the most striking derivative was Cys^{23}(13−64)-NCp7 since both ϕ_0 and $\phi_{1,1}$ were significantly lower than those of (13−64)NCp7. The photophysical basis of this phenomenon is currently under investigation.

Determination of NCp7 Binding Parameters from Fluorescence Intensity Changes: Theory. To relate the binding parameters of NCp7 derivatives containing two zinc finger motifs to the fluorescence intensity changes, we used the binding scheme in Figure 2. P, PZn^1, PZn^2, and PZn_2 corresponded to the peptide with no bound zinc, zinc bound to the N-terminal site, zinc bound to the C-terminal site, or zinc bound to both, respectively. I_0 to I_3 were the fluorescence intensities associated to the various species, while k_1 to k_4 corresponded to the experimental microscopic association constants. At any zinc concentration, the measured fluorescence intensity, I, is given by

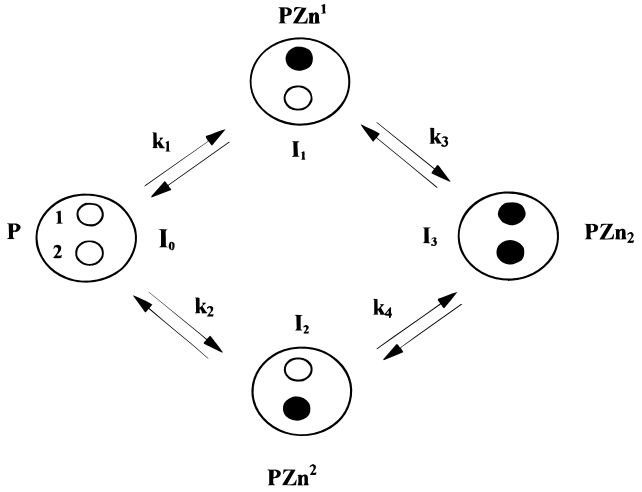

FIGURE 2: Zinc binding scheme of NCp7. Sites 1 and 2 correspond to the N- and C-terminal zinc binding motifs, respectively. Zinc-free and zinc-saturated finger motifs are represented by open and closed circles, respectively. Free zinc ions are omitted in the figure but are included in the expressions for the binding constants.

$$I = I_0\frac{[P]}{[P_T]} + I_1\frac{[PZn^1]}{[P_T]} + I_2\frac{[PZn^2]}{[P_T]} + I_3\frac{[PZn_2]}{[P_T]} \quad (1)$$

As I_0 and I_3, corresponding to the fluorescence of the apopeptide and the holopeptide, respectively, were easily measurable, we readily deduced from eq 1 the following relation

$$\Delta I = \Delta I_1\frac{[PZn^1]}{[P_T]} + \Delta I_2\frac{[PZn^2]}{[P_T]} + \frac{[PZn_2]}{[P_T]} \quad (2)$$

with $\Delta I_i = (I_i - I_0)/(I_3 - I_0)$.

Since the intrinsic fluorescent reporter for zinc binding was either Trp^{16} or Trp^{37} in the proximal and distal CCHC motifs, respectively, and since the similar low quantum yield of Trp in an apofinger motif of a related NC protein has been shown to be related to an efficient dynamic quenching process by quenchers (such as peptide carbonyl groups, protonated His, Cys sulfhydryl groups, ...) located in the finger motif sequence itself (Mély et al., 1993a), we reasonably assume that the saturation of the Trp-lacking finger by zinc does not modify the fluorescence of Trp in the neighboring random-coil apofinger motif. Therefore, we readily infer that either ΔI_1 or ΔI_2 was nil in Trp^{37}- and Trp^{16}-containing derivatives, respectively.

Moreover, using a Ser^{28}(12−53)NCp7 derivative where the affinity of the Trp-lacking proximal finger has been significantly decreased, we have shown that the fluorescence of Trp in the holofinger motif is similar to that of the (34−51)NCp7 single finger-containing derivative and thus is not affected by the neighboring Trp-lacking apofinger motif (Mély et al., 1994). In the present study, a similar conclusion holds true for Ser^{28}(13−64)NCp7 containing the additional Trp^{61} residue. Hence, we deduce that ΔI_1 and ΔI_2 were given by $\Delta I_i = (\phi_{1,0} - \phi_0)/(\phi_{1,1} - \phi_0)$, where $\phi_{1,0}$ designates the quantum yield of the corresponding isolated holofinger motif or the arithmetic mean between the quantum yield of this motif and the (51−72)peptide for Trp^{61}-lacking or Trp^{61}-containing derivatives, respectively. As demonstrated above, $\phi_{1,0} = \phi_{1,1}$ and thus $\Delta I_i = 1$ for derivatives with non-interacting fingers, whereas, due to the interaction of Trp^{16}

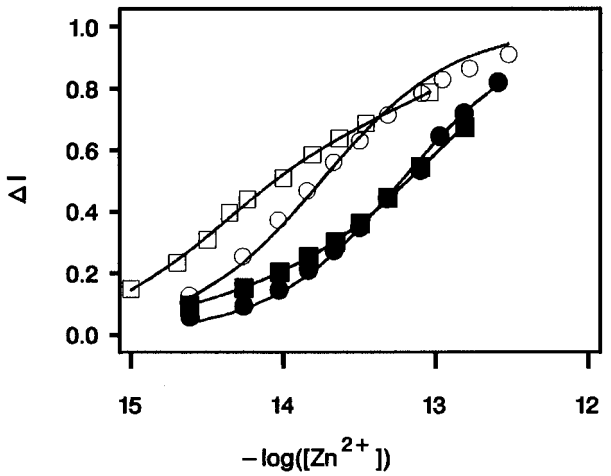

FIGURE 3: Zinc binding isotherms of NCp7 derivatives. (1−72) NCp7 (■), Trp[16]Phe[37]Phe[61](13−64)NCp7 (□), Trp[16](13−30)NCp7 (○), and (34−51)NCp7 (●) were 10 μM in 50 mM Hepes, 0.1 M KCl, 1 mM EDTA, pH 7.5. Closed and open symbols correspond to Trp[37]- and Trp[16]-containing derivatives, respectively. The solid lines were drawn by using eq 3 and the experimental binding constants of Table 1. Error bars are within experimental point symbols.

or Trp[37] with the neighboring holofinger motif, $\phi_{1,0} > \phi_{1,1}$ and thus $\Delta I_i > 1$ (Table 1) for derivatives with interacting fingers.

Using these measured or deduced ΔI_i values, we may finally deduce from eq 2 and from the basic equations relating the concentrations of the various species to the association binding constants the following equation:

$$\Delta I = \frac{\Delta I_i k_i [\mathrm{Zn}] + k_1 k_3 [\mathrm{Zn}]^2}{1 + (k_1 + k_2)[\mathrm{Zn}] + k_1 k_3 [\mathrm{Zn}]^2} \qquad (3)$$

with $i = 1$ for Trp[16]- containing derivatives and $i = 2$ for Trp[37]-containing derivatives.

Zinc Binding Parameters of NCp7 Derivatives. Using EDTA to buffer very low concentrations of free zinc, we determined the three independent binding constants, k_1 to k_3 (Table 1), from the binding isotherms (Figure 3). The fourth binding constant, k_4, which is easily derived from the other ones by $k_4 = k_1 k_3 / k_2$, was not reported. As the binding of zinc to the proximal motif only marginally affected the fluorescence of Trp[37] in the distal motif, the binding constant, k_1, of the proximal motif was correlated to k_2 and k_3 values and was less confidently determined than the uncorrelated k_2 and k_3 constants from a single titration of a Trp[37]-containing derivative. To minimize the error in k_1, the zinc titrations of each derivative were performed with various peptide concentrations and the binding constants were given as means (± standard error of the mean) for at least three experiments. The same reasoning held true for k_2 values recovered from the titration of the Trp[16]-containing derivatives.

The zinc binding isotherm of Trp[16]Phe[37]Phe[61](13−64)-NCp7 was significantly shifted toward low free zinc concentrations as compared to the isolated N-terminal finger motif (Figure 3) due to a 2-fold increase in k_1. The k_1 increase was even higher, amounting to about 5-fold for derivatives with a complete N-terminal chain: (1−72)NCp7 and (1−55)NCp7. In contrast, a 10-fold decrease of k_1 as compared to the wild-type was induced by the His[23]→Cys substitution. Concerning the distal CCHC motif, a twofold increase of k_2, as compared to the isolated (34−51)NCp7 distal finger motif, was observed for the various (13−64)-NCp7 derivatives whereas a 3-fold increase was found for (1−72)NCp7. In contrast, (12−53)NCp7, Tyr[16](12−53)-NCp7, and (1−55)NCp7 gave unchanged k_2 values. The binding isotherm of Ser[28](13−64)NCp7 was very close to the isolated C-terminal finger isotherm and was adequately fitted with a single binding parameter. Using three parameters to adjust the data did not improve the fit and gave meaningless values. Moreover, by setting different k_1 values and comparing the goodness of the fit, we found a 1×10^{12} M^{-1} upper bound limit for k_1.

From the comparison of k_2 and k_3 for Trp[37]-containing derivatives or k_1 and k_4 for Trp[16]-containing derivatives, a negative cooperativity was observed in all derivatives except D-Pro[31](13−64)NCp7 and Cys[23](13−64)NCp7. To further characterize the various derivatives, the free energy of interaction between the two sites, $\Delta\Delta G$, was calculated according to $\Delta\Delta G = -RT \ln(k_3/k_2) = -RT \ln(k_4/k_1)$. At 20 °C, the strongest effect of zinc binding to one motif on the free energy of zinc binding to the other one was observed for the complete (1−72)NCp7 protein. In contrast, $\Delta\Delta G$ was at least 2-fold lower in most other derivatives, nil in D-Pro[31](13−64)NCp7, and of opposite sign in Cys[23](13−64)NCp7.

Stoichiometric Titrations. As a final check of the consistency of the binding constants reported in Table 1, zinc titrations of NCp7 derivatives, at a concentration of 10 μM, were performed in the absence of EDTA. In these conditions, due to the very high binding constants, the binding was clearly stoichiometric. These titrations constituted a powerful check, since the filling of both finger motifs depended only on the ratio of the binding constants and possible artifacts arising from competition with EDTA disappeared. To generate the theoretical stoichiometric binding curves, we first calculated, using eq 3 and the parameters of Table 1, the ΔI values for a range of free zinc concentration [Zn]. We then calculated for the same [Zn] range the ratio, r, of total zinc to total protein concentrations using

$$r = [\mathrm{Zn}][1 + ([\mathrm{P_T}](k_1 + k_2 + 2k_1 k_3 [\mathrm{Zn}])/(1 + (k_1 + k_2)[\mathrm{Zn}] + k_1 k_3 [\mathrm{Zn}]^2))] \qquad (4)$$

The binding curves obtained from the set of (r, ΔI) values were then compared to the experimental points of the stoichiometric titrations of Trp[16]- or Trp[37]- containing derivatives. A very strong fit was observed (Figure 4) for Trp[16]Phe[37]Phe[61](13−64)NCp7, (12−53)NCp7, and Cys[23]-(13−64)NCp7, confirming the validity of our binding model and the ratios of k_i values.

pH-Dependence of the Zinc Binding Parameters. To further investigate the zinc binding properties, the pH-dependence of the binding constants of the two isolated 18-residue finger motifs was studied. An extremely sharp pH-dependence in the range 5−9 was observed for both derivatives (Figure 5). Since both Cys and His residues could be protonated in this pH range, they were likely candidates for this pH-dependence. Assuming that (i) only species with fully deprotonated Cys and His could bind zinc with a high binding constant, k_{Me}, (ii) His protonated with

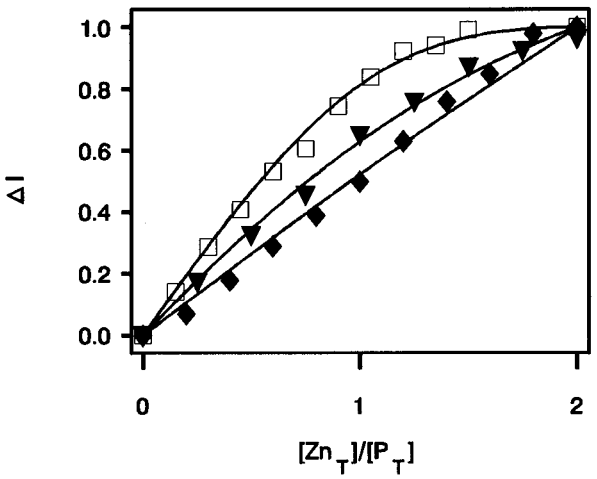

FIGURE 4: Stoichiometric titrations of NCp7 derivatives. Trp[16]-Phe[37]Phe[61](13−64)NCp7 (□), (12−53)NCp7 (♦), and Cys[23](13−64) (▼) were 10 μM in the same buffer as in Figure 3 but without EDTA. Closed and open symbols have the same meanings as in Figure 3. The solid lines were drawn as described in the text, using the k_i values of Table 1. Error bars are within experimental point symbols.

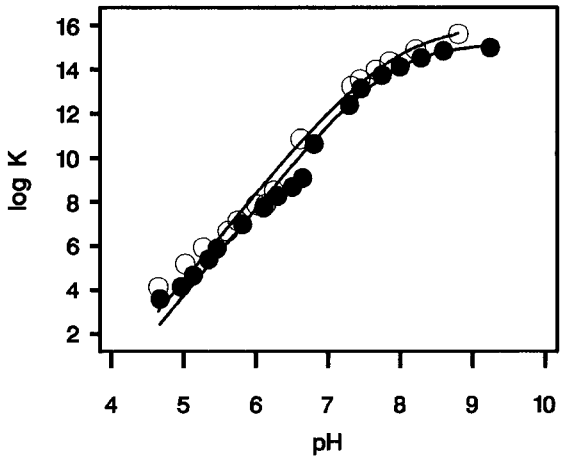

FIGURE 5: pH-dependence of the zinc binding parameters. The binding constants of Trp[16](13−30)NCp7 (○) and (34−51)NCp7 (●) were measured at different pH, as described under Materials and Methods. The solid lines were drawn by using eq 5 and the parameters of Table 2. Error bars are within experimental point symbols.

a pK_1 constant, and (iii) each Cys protonated with an identical pK_2 constant, the experimental binding constant, k, could be expressed as

$$\log(k) = \log(k_{Me}) - 3\log(1 + 10^{pK_2} \times [H]) - \log(1 + 10^{pK_1} \times [H]) \quad (5)$$

The k_{Me}, pK_1, and pK_2 values are reported in Table 2. The pK of Cys residues was identical in both peptides and close to that usually found in proteins, whereas the pK of His was not accurate enough to conclude. Noticeably, the inclusion of additional zinc binding species (e.g., monoprotonated ones) in eq 5 did not improve the fit, validating the hypothesis that, as for the MoMuLV NC (Mély et al., 1991) or the yeast transcription factor zinc finger domains (Parraga et al., 1990), only species with fully deprotonated His and Cys bind zinc strongly.

To determine the influence of pH on the zinc binding constants of NCp7 derivatives containing two finger motifs,

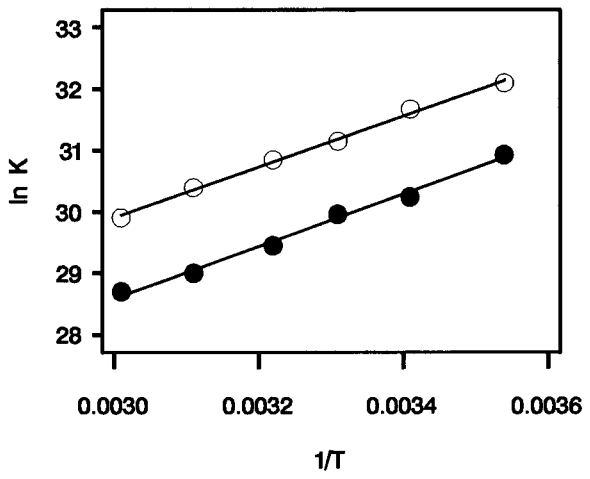

FIGURE 6: van't Hoff plots for the association of zinc to CCHC motifs. Peptides and symbols were as in Figure 5. The linear fits were obtained with the $\Delta H°$ and $\Delta S°$ values of Table 2.

Table 2: pH- and Temperature-Dependence of the Zinc Binding Parameters of the Isolated Zinc Finger Motifs[a]

	k_{Me}	pK_1	pK_2	$\Delta H°$ (kJ/mol)	$\Delta S°$ (J/K/mol)
Trp[16](13−30) NCp7	8 (±3) × 10^{15}	8.17 (±0.08)	6.9 (±0.5)	34 (±3)	148 (±8)
(34−51)NCp7	2 (±1) × 10^{15}	8.04 (±0.07)	7.3 (±0.3)	35 (±1)	130 (±8)

[a] Binding constants and thermodynamic parameters were defined in the text and were expressed as means (± standard error of the mean) for at least three experiments.

Table 3: Zinc Binding Constants of NCp7 Derivatives at pH 7.0[a]

	k_1 (M^{-1})	k_2 (M^{-1})	k_3 (M^{-1})	$\Delta\Delta G$ (kJ/mol)
Trp[16]Phe[37]Phe[61] (13−64)NCp7	7.9 (±0.4) × 10^{12}	3 (±2) × 10^{12}	1.0 (±0.3) × 10^{12}	2.7
(12−53)NCp7	7 (±3) × 10^{12}	8 (±2) × 10^{11}	4.8 (±0.4) × 10^{11}	1.2

[a] Binding parameters were determined and expressed as in Table 1.

the zinc binding properties of Trp[16]Phe[37]Phe[61](13−64)NCp7 and (12−53)NCp7 were investigated at pH 7.0. In good keeping with the isolated zinc finger motifs, a strong decrease in both k_1 and k_2 (Table 3) as compared to pH 7.5 was observed in both derivatives. Moreover, as at pH 7.5, the binding of zinc to one motif decreased the affinity of zinc for the second motif and the free energy of interaction between the two sites was indistinguishable from that at pH 7.5.

Temperature-Dependence of the Zinc Binding Parameters. To get further insight in the zinc binding mechanism, the temperature-dependence of Trp[16](13−30)NCp7 and (34−51)-NCp7 zinc binding constants was studied at pH 7.5 over the 10−60 °C range. To ensure that the peptides were still fully saturated with zinc at the highest temperature, a further 10-fold molar excess of zinc was added at this temperature. No change in fluorescence intensity was observed in either peptide, suggesting that both peptides were still in their holoforms. Furthermore, at the end of the experiment, when the peptides were cooled down to 20 °C, the fluorescence intensity returned to its initial value before heating. This suggests that no irreversible denaturation of the peptides occurred during the heating process.

Plotting the logarithm of the experimental binding constant versus the reciprocal of the temperature in a van't Hoff plot

(Figure 6) gave a straight line, suggesting that the change in heat capacity, $\Delta C_p°$, with temperature is nil or is very low. From linear least-squares fits, we deduced the enthalpy changes, $\Delta H°$, and entropy changes, $\Delta S°$, given in Table 2. Whereas $\Delta H°$ was similar in both fingers, $\Delta S°$ was about 15% higher in the N-terminal finger motif.

DISCUSSION

As in many other retroviruses, the HIV-1 nucleocapsid protein NCp7 is characterized by two CCHC zinc finger motifs. Using the fluorescence of either the naturally occurring Trp^{37}, located in the C-terminal finger motif or the conservatively substituted Trp^{16} in the N-terminal finger motif, the zinc binding properties of both fingers could be selectively investigated.

The zinc binding constants of two 18-residue synthetic peptides with the amino acid sequence of the isolated N- or C-terminal finger motifs were close to those in the whole NCp7 protein, suggesting that, as for the related NC of MoMuLV (Mély et al., 1993a), the finger motifs possess most of the information necessary and sufficient to strongly bind zinc. In keeping with the previously suggested differences in the zinc binding properties of the two motifs (De Rocquigny et al.,1991; Fitzgerald & Coleman, 1991), a 3-fold higher affinity, related to an increased entropic contribution, was observed for the N-terminal versus the C-terminal binding motif at pH 7.5. Surprisingly, in both zinc finger motifs, the entropy changes contributed more than half of the zinc binding free energy, despite the transition from a random-coil to a highly constrained structure induced by the binding of zinc (Summers, 1991). Hence, this unfavorable structural entropy must be overcome by a very strong favorable entropic contribution due to loss of hydration water from both the zinc ion (Atkins, 1990) and the rearrangement of the highly hydrophilic peptide motifs during complexation. This latter point was confirmed by the comparison, from computational simulation in a water bath, of the extended peptides corresponding to the apoforms of the finger motifs on one hand and the NMR-derived solution structure of the zinc-saturated (12−53)NCp7 on the other hand. This comparison revealed that the CCHC motifs in the highly constrained (12−53)NCp7 holopeptide bound 30%−40% less H_2O molecules (through hydrogen bond) than the apopeptides.

The comparison of the zinc binding constants of various NCp7 derivatives suggested that both the N- and C-terminal chains surrounding the zinc finger motifs domain increased the zinc binding free energy of the proximal and distal CCHC motifs, respectively, by about 1−4 kJ/mol. The highest binding constants were observed for the entire (1−72)NCp7, suggesting a slightly improved stability of the major cleavage product of the BH10 isolate versus (1−55)NCp7, the major cleavage product of the MN isolate. Moreover, from the data of (12−53)NCp7, the shortest NCp7 derivative containing the two finger motifs, we inferred that a CCHC finger motif in its apoform was without effect on the zinc binding affinity of the neighboring one. In contrast, when one motif was saturated with zinc, the binding constant of the remaining one decreased up to 4-fold. This negative cooperativity and the corresponding free energy of interaction between the binding sites were clearly related to the spatial proximity of the finger motifs since they vanished in both D-Pro^{31}(13−64)NCp7 and Cys^{23}(13−64)NCp7 where the finger motifs have been shown to be no more in close contact (Déméné et al., 1994; Morellet et al., 1994).

As expected, the Cys and His ligands of the CCHC motifs played a critical role in the zinc binding properties. Substitution of Cys^{28} even by a Ser residue markedly decreased the affinity of the proximal finger motif by at least 2 orders of magnitude. This decrease might prevent the saturation of the proximal finger by zinc in intracellular conditions and hence induce the previously observed impairment in viral RNA content and virus replication (Dorfman et al., 1993). Alternatively, as the quantum yield of Ser^{28}(13−64)NCp7 in the presence of an excess of zinc was identical to that of derivatives with non-interacting fingers, the substitution of Cys^{28} by Ser might prevent the spatial proximity of the two CCHC motifs and thus hinder the correct recognition of the homologous RNA.

More unexpectedly, as Cys has been reported to be a stronger zinc ligand than His (Vallee & Auld, 1990), the His^{23}→Cys substitution in the N-terminal finger motif induced a 10-fold decrease in the zinc binding constant of this site. This affinity decrease probably arose from the important structural alterations induced by this mutation (Déméné et al., 1994) but was probably too weak to induce the observed loss of virion infectivity. In fact, this loss of infectivity seems to be related to the structural alteration in the zinc-saturated mutated finger motif and/or the impairment of the spatial proximity between the finger motifs (Déméné et al., 1994; Mély et al., 1994).

In contrast to Cys and His residues, the nature of the highly conserved aromatic amino acid immediately following the first Cys residue in the CCHC finger motif did not appeared to be critical for zinc binding. Hence, the slight reduction in viral infectivity and packaging, observed when Phe^{16} and Trp^{37} were inverted (data not shown), was probably related to the minimal structural changes induced by this inversion.

Moreover, we showed that the binding of zinc to the isolated or associated finger motifs was exquisitely pH-dependent due to competition between zinc and protons for the Cys and His ligands. Careful analysis of this pH-dependence revealed that the proximal CCHC motif essentially differed from the distal one by a 4-fold higher intrinsic association binding constant, k_{Me}, associated to the species with fully deprotonated ligands. Both this steep pH-dependence and the somewhat lower entropy of the binding of zinc to the C-terminal finger motif might be responsible of the temperature-dependent lability of this motif observed by ^1H NMR at lower pH (South et al., 1991; Morellet et al., 1992).

In conclusion, our data on the zinc binding properties of NCp7 clearly confirmed the nonequivalence of the two CCHC finger motifs, in keeping with the previously reported differences in structure and thermal stability (South et al., 1991; Omichinski et al., 1991; Morellet et al., 1992; Summers et al., 1992; Mély et al., 1993b). Moreover, the characterization of the zinc binding scheme of NCp7 allows one to rationally quantify now the effects of zinc competitors which have been reported to represent a putative new approach to the chemotherapy of AIDS (Rice et al., 1993).

ACKNOWLEDGMENT

We are indebted to M. C. Fournié-Zaluski for stimulating discussion and to M. Wernert for her expert editorial assistance.

REFERENCES

Aldovini, A., & Young, R. A. (1990) *J. Virol. 64*, 1920−1926.
Atkins, P. W. (1990) in *Physical Chemistry*, Plenum Press, New York.
Barat, C., Lullien, V., Schatz, O., Keith, G., Nugeyre, M. T., Grüninger-Leitch, F., Barré-Sinoussi, F., Le Grice, S. F. J., & Darlix, J. L. (1989) *EMBO J. 8*, 3279−3285.
Barat, C., Le Grice, S. F. J., & Darlix, J. L. (1991) *Nucleic Acids Res. 19*, 751−757.
Berg, J. M. (1986) *Science 232*, 485−487.
Berkowitz, R. D., & Goff, S. P. (1994) *Virology 202*, 233−246.
Berkowitz, R. D., Luban, J., & Goff, S. P. (1993) *J. Virol. 67*, 7190−7200.
Bess, J. W., Jr., Powell, P. J., Issaq, H. J., Schumack, L. J., Grimes, M. K., Henderson, L. E., & Arthur, L. O. (1992) *J. Virol. 66*, 840−847.
Blinks, J. R., Wier, W. G., Hess, P., & Prendergast, F. G. (1982) *Prog. Biophys. Mol. Biol. 40*, 1−114.
Clever, J., Sassetti, C., & Parslow, T. G. (1995) *J. Virol. 69*, 2101−2109.
Cornille, F., Mély, Y., Ficheux, D., Savignol, I., Gérard, D., Darlix, J. L., Fournié-Zaluski, M. C., & Roques, B. P. (1990) *Int. J. Peptide Protein Res. 36*, 551−558.
Dannull, J., Surovoy, A., Jung, G., & Moelling, K. (1994) *EMBO J. 13*, 1525−1533.
Darlix, J. L., Gabus, C., Nugeyre, M. T., Clavel, F., & Barré-Sinoussi, F. (1990) *J. Mol. Biol. 216*, 689−699.
Darlix, J. L., Lapadat-Tapolsky, M., De Rocquigny, H., & Roques, B. P. (1995) *J. Mol. Biol. 254*, 523−537.
De Rocquigny, H., Ficheux, D., Gabus, C., Fournié-Zaluski, M. C., Darlix, J. L., & Roques, B. P. (1991) *Biochem. Biophys. Res. Commun. 180*, 1010−1018.
De Rocquigny, H., Gabus, C., Vincent, A., Fournié-Zaluski, M. C., Roques, B., & Darlix, J. L. (1992) *Proc. Natl. Acad. Sci. U.S.A. 89*, 6472−6476.
Déméné, H., Dong, C. Z., Ottmann, M., Rouyez, M. C., Jullian, N., Morellet, N., Mély, Y., Darlix, J. L., Fournié-Zaluski, M. C., Saragosti, S., & Roques, B. P. (1994) *Biochemistry 33*, 11707−11716.
Dorfman, T., Luban, J., Goff, S. P., Haseltine, W. A., & Göttlinger, H. G. (1993) *J. Virol. 67*, 6159−6169.
Eisinger, J., & Navon, G. (1969) *J. Chem. Phys. 50*, 2069−2077.
Fitzgerald, D. W., & Coleman, J. E. (1991) *Biochemistry 30*, 5195−5201.
Gorelick, R. J., Nigida, S. M., Bess, J. W., Jr., Arthur, L. O., Henderson, L. E., & Rein, A. (1990) *J. Virol. 64*, 3207−3211.
Gorelick, R. J., Chabot, D. J., Rein, A., Henderson, L. E., & Arthur, L. O. (1993) *J. Virol. 67*, 4027−4036.
Green, L. M., & Berg, J. M. (1990) *Proc. Natl. Acad. Sci. U.S.A. 87*, 6403−6407.
Karpel, R. L., Henderson, L. E., & Oroszlan, S. (1987) *J. Biol. Chem. 262*, 4961−4967.
Lapadat-Tapolsky, M., De Rocquigny, H., Van Gent, D., Roques, B., Plasterk, R., & Darlix, J. L. (1993) *Nucleic Acids Res. 21*, 831−839.
Lapadat-Tapolsky, M., Pernelle, C., Borie, C., & Darlix, J. L. (1995) *Nucleic Acids Res. 23*, 2434−2441.
Martell, A. E., & Smith, R. M. (1974) in *Critical Stability Constants*, Vol. 1, pp 204−211, Plenum Press, New York.
Mély, Y., Cornille, F., Fournié-Zaluski, M. C., Darlix, J. L., Roques, B. P., & Gérard, D. (1991) *Biopolymers 31*, 899−906.
Mély, Y., De Rocquigny, H., Piémont, E., Déméné, H., Jullian, N., Fournié-Zaluski, M. C., Roques, B. P., & Gérard, D. (1993a) *Biochim. Biophys. Acta 1161*, 6−18.
Mély, Y., Piémont, E., Sorinas-Jimeno, M., De Rocquigny, H., Jullian, N., Morellet, N., Roques, B. P., & Gérard, D. (1993b) *Biophys. J. 65*, 1513−1522.
Mély, Y., Jullian, N., Morellet, N., De Rocquigny, H., Dong, C. Z., Piémont, E., Roques, B., & Gérard, D. (1994) *Biochemistry 33*, 12085−12091.
Morellet, N., Jullian, N., De Rocquigny, H., Maigret, B., Darlix, J. L., & Roques, B. P. (1992) *EMBO J. 11*, 3059−3065.
Morellet, N., De Rocquigny, H., Mély, Y., Jullian, N., Déméné, H., Ottmann, M., Gérard, D., Darlix, J. L., Fournié-Zaluski, M. C., & Roques, B. P. (1994) *J. Mol. Biol. 235*, 287−301.
Omichinski, J. G., Clore, G. M., Sakaguchi, K., Appella, E., & Gronenborn, A. M. (1991) *FEBS Lett. 292*, 25−30.
Ottmann, M., Gabus, C., & Darlix, J. L. (1995) *J. Virol. 69*, 1778−1784.
Parraga, G., Horvath, S., Hood, L., Young, E. T., & Klevit, R. E. (1990) *Proc. Natl. Acad. Sci. U.S.A. 87*, 137−141.
Rice, W. G., Schaeffer, C. A., Harten, B., Villinger, F., South, T. L., Summers, M.F., Henderson, L. E., Bess, J. W., Jr., Arthur, L. O., McDougal, J. S., Orloff, S. L., Mendeleyev, J., & Kun, E. (1993) *Nature 361*, 473−475.
Sakaguchi, K., Zambrano, N., Baldwin, E. T., Shapiro, B. A., Erickson, J. W., Omichinski, J. G., Clore, G. M., Gronenborn, A. M., & Appella, E. (1993) *Proc. Natl. Acad. Sci. U.S.A. 90*, 5219−5223.
Sheng, N., & Erickson-Viitanen, S. (1994) *J. Virol. 68*, 6207−6214.
South, T. L., Blake, P. R., Hare, D. R., & Summers, M. F. (1991) *Biochemistry 30*, 6342−6349.
Summers, M. F. (1991) *J. Cell. Biochem. 45*, 41−48.
Summers, M. F., Henderson, L. E., Chance, M. R., Bess, J. W., Jr., South, T. L., Blake, P. R., Sagi, I., Perez-Alvarado, G., Sowder, R. C., III, Hare, D. R., & Arthur, L.O. (1992) *Protein Sci. 1*, 563−574.
Vallee, B. L., & Auld, D. S. (1990) *Biochemistry 29*, 5647−5659.

BI952587D